ELSEVIER

Polymer 40 (1999) 1299–1304

polymer

On the particulate structure of cellulose solutions

Bernd Morgenstern[a,*], Hans-Werner Kammer[b]

[a]*Technische Universität Dresden, Institut für Physikalische Chemie und Elektrochemie, D-01062 Dresden, Germany*
[b]*Universiti Sains Malaysia, School of Chemical Sciences, 11800 Penang, Malaysia*

Received 9 December 1997; revised 25 March 1998; accepted 25 March 1998

Abstract

A simple model for aggregate formation in cellulose solutions is presented. Owing to a strong tendency of hydrogen-bond formation among the cellulose molecules, aggregation does not lead to a completely random arrangement of the molecules. In a core, parts of the chain molecules are laterally aligned. This core is surrounded by disordered regions that give rise to the formation of coronas under the action of solvent molecules while the core is completely immiscible with the solvent. Therefore, the aggregates can be seen as fringed micelles. The equilibrium structure of these micelles, number of aggregated chains and size of the coronas, is discussed as a function of the interfacial tension between core and solvent. It turns out that both number of aggregated chains and thickness of the coronas increase with increasing interfacial tension. In perfect solutions of the micelles, these quantities also increase with cellulose concentration. If one admits attractions between coronas of different micelles, as a small perturbation, clustering of micelles might be induced. This may cause phase instability of the particle phase which results in the coexistence of a diluted and a more concentrated solution.

Keywords: Cellulose solution; Fringed micelle; Phase stability

1. Introduction

Dissolution of cellulose has been studied extensively over the last two decades, and a variety of solvent systems is known [1–4]. For many of those solvent systems, it turns out, however, that dissolution of cellulose cannot be done in one step since the highly ordered structure of native cellulose prevents access of solvent molecules. Then, prior to dissolution, in a process of activation, the ordered (crystalline) domains of cellulose are transferred in disordered regions. Concomitantly, the hydrogen-bond system of cellulose is disintegrated to some extent. These alterations of the cellulose structure turn out to be prerequisites for the solvent molecules to get access to the cellulose chains. Usually, activation is carried out by swelling of cellulose in a highly polar medium or by thermo-mechanical treatments. There are also reports on enzymatically controlled and radiation-induced activation procedures [5,6].

However, this activation process may not disintegrate completely the ordered domains of cellulose. As a result, cellulose solutions cannot be seen as molecularly dispersed systems, but comprise aggregates of still ordered cellulose molecules. This seems to be a characteristic pattern of cellulose solutions [7]. For solutions of incompletely substituted cellulose derivatives, it was suggested that these aggregates consist of a core of aligned chains with coronas of dangling chains at the ends [7,8]. Scattering experiments revealed that the linear mass density of the aggregates increases with weight-average molecular weight, concomitantly, the objects become stiffer. This increase of linear mass density and the accompanying increase of chain stiffness give direct evidence for lateral aggregation of the chains [7]. Here, we adopt this model of fringed micelles as the state of aggregation in cellulose solutions. Moreover, we focus on a special class of solvent systems. Common features of these systems are: they all consist of an aprotic polar solvent (e.g. dimethylacetamide) in combination with an inorganic salt, preferably lithium chloride (LiCl). There is experimental evidence that LiCl ion pairs form complexes with the polar solvent molecules [9–12]. Obviously, these complexes play a prominent role in dissolving of cellulose [1,4,11,13,14]. The study opens with a discussion on the stability of fringed micelles. This is followed by outlines on solutions of such aggregates.

2. Model

2.1. Fringed micelles of cellulose molecules

The ternary solution composed of cellulose chains with a

* Corresponding author: Tel: 0049 351 463 4609; Fax: 0049 351 463 7164.

0032-3861/98/$ - see front matter
PII S0032-3861(98)00267-5

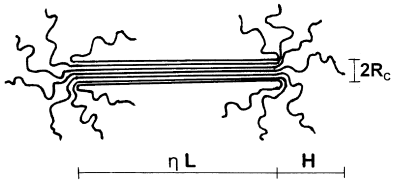

Fig. 1. Fringed micelle (cf. text).

degree of polymerization N_C, an inorganic salt and a polar organic solvent is seen as a quasi-binary system of cellulose molecules and solvent complexes formed by solvent molecules and the salt. This can be done as long as the concentrations of cellulose and salt are small compared with the concentration of the organic solvent in the ternary system. Moreover, it is assumed that any salt molecule forms a complex with solvent molecules. Then, the volume fractions of cellulose Φ and complexes Φ_{compl} are given by

$$\Phi = \frac{N_C N_{cell}}{N} \text{ and } \Phi_{compl} = \frac{N_{compl}}{N} \tag{1}$$

where N_{cell} and N_{compl} are the numbers of cellulose molecules and solvent complexes, respectively, and N is the total number of monomers in the system, $N = N_C N_{cell} + N_{compl}$.

Now, we assume that the cellulose solution consists of aggregates, each of which comprises p cellulose molecules. As mentioned earlier, cellulose is not completely amorphous after the activation procedure. This implies that there still exist ordered domains surrounded by amorphous regions. The ordered domains are completely immiscible with the solvent while for the amorphous regions the solvent complexes turn out to be a moderate solvent. One may say, the driving force for formation of highly ordered aggregate cores is to establish a regular network of hydrogen bonds between the aligned cellulose molecules and to reduce the unfavourable contacts with the solvent complexes. The aggregates, that develop under the action of the solvent complexes, are supposed to be of the type of fringed micelles with a cylindrical core that splits in spherical coronas at both ends (cf. Fig. 1). To surface sites of the core, that are able to form hydrogen bonds, solvent complexes are attached. This governs the core's interfacial tension, $K k_B T$ (k_B, Boltzmann's constant; T, absolute temperature), to the surrounding medium. Solvent complexes are only adsorbed at the cylindrical core.

The free energy of a single aggregate, composed of p cellulose molecules, is an important quantity for studying the properties of the solution. Now, we assume that the chains are perfectly aligned in the core forming without the coronas a circular cylinder with the chain ends in the basal planes. This is certainly an idealized form of the aggregates. The contour length of one cellulose molecule is L. If η characterizes the part of the molecule within the core, its length is given by $\eta L = a\eta N_C$ where a denotes the length of one monomer unit. The rest of the molecules forms spherical coronas at the ends of the core. The diameter of one cellulose molecule is d then the radius of the core, R_c, is

$$R_c = p^{1/2}\frac{d}{2} \tag{2}$$

The free energy of a single aggregate may be approximated by a sum of two contributions, arising from the special structure of the micelle

$$\Delta F_{single} = \Delta F_{interface} + \Delta F_{corona} \tag{3}$$

The first term represents the interfacial free energy of the core. With Eq. (2), it reads

$$\Delta F_{interface}/k_B T = \pi\eta p^{1/2} K a^2 \left(\frac{d}{a}\right) N_C \tag{4}$$

The second term stands for the coronal energy. Following Halperin [15], we formulate this contribution in terms of blobs, i.e. chain parts that display single chain behaviour. It results in

$$\frac{\Delta F_{corona}}{k_B T} \cong 2p^{3/2}\ln\left[\frac{R_C + H}{R_C}\right] \cong 2\nu p^{3/2} \times \ln\left[1 + \frac{2^{1/\nu - 1}}{\nu}\left(\frac{a}{d}\right)^{1/\nu}\frac{(1-\eta)N_C}{p^{1/2}}\right] \tag{5}$$

where H is the thickness of the corona and ν is the single chain exponent, $\nu = 1/2$ for an ideal chain and $\nu = 3/5$ for a chain in a good solvent. Details of derivation of Eq. (5) are given in Appendix A. For $R_c \ll H$ and $\eta > (1 - \eta)$, the thickness of the corona might be approximated by

$$H = \frac{a(1-\eta)^\nu N_C^\nu}{(2\nu)^\nu p^{(\nu-1)/2}} \approx \frac{a}{(2\nu)^\nu}\frac{N_C^\nu}{p^{(\nu-1)/2}} \tag{6}$$

Eq. (5) is not correct anymore in the limits $\eta \to 1$ and $\eta < (1 - \eta)$, respectively. In the first case, the corona is not spherical but consists of stretched chains while in the second case overlapping of the coronas occurs.

Minimization of the free energy, Eq. (3), per aggregated chain results in two equations for quantities p and η and yields the equilibrium structure of a single micelle. With Eqs. (4) and (5), it follows

$$1 - \eta = \frac{1}{q}\frac{p^{1/2}}{N_C}\left[\frac{2^{1/\nu}}{\pi}\left(\frac{a}{d}\right)^{1/\nu+1}\frac{p^{1/2}}{Ka^2} - 1\right] \text{ and}$$

$$Ka^2 = \frac{2\nu}{\pi}\left(\frac{a}{d}\right)\frac{p}{N_C}\ln\left[\frac{2^{1/\nu}}{\pi}\left(\frac{a}{d}\right)^{1/\nu+1}\frac{p^{1/2}}{Ka^2}\right] \tag{7}$$

where

$$q \equiv \frac{2^{1/\nu - 1}}{\nu}\left(\frac{a}{d}\right)^{1/\nu}$$

From Eqs. (7) one gets the following rough approximations for the dependencies of p and η on Ka^2, in the limit $(N_C/p^{1/2}) \gg 1$

$$\frac{p}{N_C} \approx \frac{Ka^2}{\ln\left(\frac{p^{1/2}}{Ka^2}\right)} \text{ and } 1 - \eta \approx \frac{1}{\ln\left(\frac{p^{1/2}}{Ka^2}\right)} \tag{7a}$$

Since $\ln[(p^{1/2})/(Ka^2)]$ only weakly depends on Ka^2, the number of chains forming the aggregate increases almost linearly with Ka^2 whereas the length of the core only weakly changes with interfacial energy Ka^2. For very small values of Ka^2, $p/(N_C) \to 0$ and $(1-\eta) \to [1/(N_C)]$ which means the coronas disappear. In the limit of sufficiently high values of Ka^2, $\eta \to 1/2$ and the coronas start to overlap. In both situations, the model becomes meaningless.

2.2. The free energy of a perfect micellar solution

Minimization of the free energy of a single micelle, given by Eqs. (3)–(5), with respect to the quantities p and η leads only to approximate results since the quantities p and η also depend on the composition of the solution. This is so because the entropy of mixing of aggregates and free solvent complexes contributes to the free energy of the particle phase. It affects the equilibrium properties of the particle phase like the average dimension of the aggregates. For any concentration Φ of cellulose there will be an average number $p(\Phi)$ and an average reduced core length $\eta(\Phi)$.

In the first step, the system is regarded as a perfect solution of $(N\Phi)/(pN_C)$ particles and $N(1-\Phi\xi)$ mobile solvent complexes. Since each core caries $\pi\eta p^{1/2} N_C(d/a)$ immobile solvent complexes, the quantity ξ reads

$$\xi = 1 + \frac{\pi\eta}{p^{1/2}}\left(\frac{d}{a}\right) \tag{8}$$

The free energy of the particle phase, with reference to the pure components, is given as the sum of two contributions

$$\Delta F = \frac{N\Phi}{pN_C}\Delta F_{\text{single}} - T\Delta S_{\text{mix}} \tag{9}$$

where ΔS_{mix} represents the entropy of mixing of the aggregates and the mobile solvent complexes. It can be expressed as

$$\frac{\Delta S_{\text{mix}}}{N k_B} = -\frac{\Phi}{pN_C}\ln(\Phi\xi) - (1-\Phi\xi)\ln(1-\Phi\xi) \tag{10}$$

Eq. (10) results if one places $(N\Phi)/(pN_C)$ particles and $N(1-\Phi\xi)$ complexes on lattice sites.

Minimization of the total free energy, Eq. (9), with respect to p and η yields the equilibrium structure of the micelles in a perfect solution. In the same rough approximation that led to Eq. (7a), the quantities p and η now read

$$\frac{p}{N_C} \approx \frac{\mathcal{K}}{\ln\left(\frac{p^{1/2}}{\mathcal{K}}\right)} \text{ and } 1-\eta \approx \frac{1}{\ln\left(\frac{p^{1/2}}{\mathcal{K}}\right)} \tag{11}$$

with

$$\mathcal{K} \equiv [Ka^2 - 1 - \ln(1-\Phi\xi)] \tag{11a}$$

The precise expressions for p and η are given in Appendix B. They are very similar to Eqs. (7) if one replaces Ka^2 by $\mathcal{K}$. Eqs. (11) and (11a) show that changes in concentration of cellulose, Φ, influence more the quantity p than the quantity η. At $Ka^2 = \text{const}$, particle number p increases with Φ while η slightly decreases. Here, we have $p/(N_C) \to 0$ and $(1-\eta) \to 1/N_C$ if $\mathcal{K} \ll 1$.

2.3. Interactions between micelles

The free energy, Eq. (9), describes a perfect solution of $(N\Phi)/(pN_C)$ micelles and $N(1-\Phi\xi)$ solvent complexes. Now we assume, the micelles of size $p(\Phi)$ and $\eta(\Phi)$ exert some interactions to each other. In the limit $(N_C)/(p^{1/2}) \gg 1$, the free energy of a perfect solution of micelles, having their equilibrium structure, can be approximated by

$$\Delta F_{\text{eq}} = \Phi Ka^2(\xi - 1) + (1-\Phi\xi)\ln(1-\Phi\xi) \tag{12}$$

according to Eqs. (5), (9) and (B3). We now allow, as a small perturbation compared with Ka^2, attractions between micelles and express the corresponding free energy as follows

$$\frac{\Delta F}{N k_B T} = \Delta F_{\text{eq}} - \beta\left(\frac{\Phi}{p^{1/2}}\right)^n \tag{13}$$

The first term of Eq. (13) is given by Eq. (12) and the second one takes into account interactions between n micelles with β being the corresponding interaction parameter. It results from $(H^2\Phi)/(pN_C)$ where H^2 has been approximated by $H^2 \cong a^2 N_C p^{1/2}$ after Eq. (6) with $\nu = 1/2$. To analyse the phase stability of a solution of interacting micelles, one has to calculate the derivatives of Eq. (13) with respect to Φ. According to Eq. (11), the parameter η can be seen as independent of Φ to a good approximation. Moreover, we assume

$$\left|\frac{d\xi}{d\Phi}\right| = \frac{\pi\eta}{p^{1/2}}\left(\frac{1}{2p}\frac{dp}{d\Phi}\right) \le \frac{\pi\eta}{p^{1/2}} \ll 1 \tag{14}$$

[cf. below, Eq. (18)]. With these approximations the second and third derivatives of Eq. (11) with respect to Φ can be represented by

$$\frac{\Delta F''}{N k_B T} = -\beta n(n-1)\frac{\Phi^{n-2}}{p^{n/2}}[1+Y] + \frac{\xi^2}{1-\Phi\xi} \tag{15}$$

$$\frac{\Delta F'''}{N k_B T} = -\beta n(n-1)(n-2)\frac{\Phi^{n-3}}{p^{n/2}}[1+Z] + \frac{\xi^3}{(1-\Phi\xi)^2} \tag{16}$$

The quantities Y and Z comprise first to third derivatives of p with respect to Φ. The explicit form of Y is given in Appendix C. From Eqs. (15) and (16), we get for the critical values of β and Φ the following expressions

$$\frac{\beta_c}{p^{n/2}\xi^n} = \frac{1}{n}\left(\frac{n-1}{n-2}\right)^{n-2}\frac{\left(1 + \frac{1}{n-1}Y + \frac{n-2}{n-1}Z\right)^{n-1}}{(1+Y)^2(1+Z)^{n-2}} \tag{17}$$

$$\xi\Phi_c = \frac{n-2}{n-1}\frac{1+Z}{\left(1 + \frac{1}{n-1}Y + \frac{n-2}{n-1}Z\right)}$$

As can be seen the smallest value for n, where phase

instability occurs, is $n = 3$. With increasing n, the critical value of parameter β increases. In the following, we consider only $n = 3$. From Eq. (B1), we can calculate the derivatives of p with respect to Φ. The first two read in the approximation $(N_C/p^{1/2}) \gg 1$ (cf. Appendix C)

$$\left(\frac{\Phi}{2p}\frac{dp}{d\Phi}\right) = \frac{1}{2\mathcal{K}}\frac{\Phi\xi}{1-\Phi\xi} \text{ and } \left(\frac{\Phi^2}{2p}\frac{d^2p}{d\Phi^2}\right) = \frac{1}{2\mathcal{K}}\left(\frac{\Phi\xi}{1-\Phi\xi}\right)^2 \tag{18}$$

where $\mathcal{K}$ is given by Eq. (11a). From Eq. (18), one sees that $\{[\Phi/(2p)][(dp)/(d\Phi)]\}$ varies between zero and approximately one for $0 \le \Phi\xi \le 0.6$ (if $Ka^2 \ne 1$) and decreases with increasing Ka^2. Approximately, the same variation shows the second derivative of p within the limits $0 \le \Phi\xi \le 0.5$.

Eq. (13) also depends on $p^{n/2}$ that varies with Φ. One gets from Eq. (B1)

$$p^{1/2} = \frac{\pi}{(2a/d)^{1/\nu+1}\mathcal{K}}\left[1+\sqrt{1+\frac{2^{2/\nu+1}(a/d)^{1/\nu+1}}{\pi\nu}\frac{(1-\eta)N_C}{\mathcal{K}}}\right] \tag{19}$$

where $\mathcal{K}$ is given by Eq. (11a). Inserting Eqs. (18) and (19) in Eq. (15) (with Y as given in Appendix C) allows to calculate stability limits for solutions of interacting micelles in the limits $(N_C/p^{1/2}) \gg 1$ and $\eta,\xi = \text{const}$.

3. Discussion

Particle number p and core length η of a single micelle as well as for micelles in perfect solutions of different cellulose concentrations are depicted in Figs 2 and 3 as functions of Ka^2. The curves were calculated from Eqs. (7), (B1) and (B2), respectively. Since we assume $(a/d) = 1$, the influence of the single chain exponent can be neglected. The results confirm the general tendencies given by Eqs. (7) and (11). With ascending interfacial energy, the number of molecules, forming the micelles, increases while η slightly decreases. The interfacial tension of the aggregates is related to the adsorption tendency of the solvent complexes to surfaces sites of the core. If this tendency is high, the interfacial

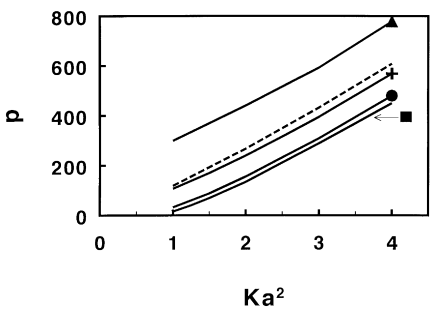

Fig. 2. Variation of number of cellulose molecules p aggregated in a micelle with interfacial energy Ka^2. The curves were calculated after Eqs. (7) for the single micelle (dashed curve) and after Eqs. (B1) and (B2) for micelles in perfect solutions with the parameters $N_C = 100$, $\nu = 1/2$ and $a/d = 1$. Cellulose concentrations Φ: 0.8 (▲); 0.5 (+); 0.2 (●); and 0.1 (■).

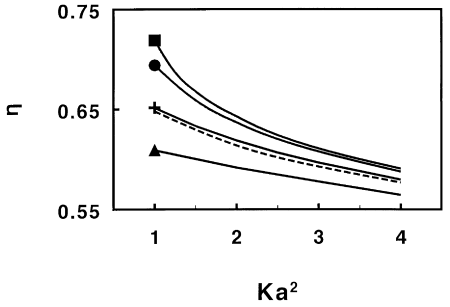

Fig. 3. Variation of reduced core length η with Ka^2. Others as in Fig. 2.

tension of the aggregate will be low and therefore, also the number of particles forming it. Formation of the ordered core corresponds to an enormous decrease in conformational entropy of the chains and can take place only if there are strong enough interactions between the chains. This ordered arrangement gradually decays in amorphous regions, surrounding it, that give rise to formation of the disordered coronas. A tendency that slightly increases with increasing particle number which results in a slight decrease of η with Ka^2. As mentioned earlier, the model becomes unrealistic in the limits of very low and high values of Ka^2 ($Ka^2 > 10$). In the former case, one approaches $p \rightarrow 1$ which is associated with $\eta \rightarrow 1$ and in the opposite case, p tends to very high values with $\eta \rightarrow 1/2$ where the coronas start to overlap.

The change of quantities p and η with cellulose concentration is depicted in Figs 4 and 5 for different values of Ka^2. Quantity η displays only slight variations with Φ, that even decrease with increasing Ka^2, while changes in p with cellulose concentration are more pronounced. Thus, the size of the aggregates increases with both with cellulose concentration and with Ka^2. The same tendency can be seen for the size of the coronas although less pronounced.

The stability of the particle solutions, we discuss in terms of Eq. (15), $(\Delta F'')/(N k_B T) = 0$, with $n = 3$. From Eq. (17), it follows that $[(\beta_c)/(p^{3/2}\xi^3)] \rightarrow 2/3$ and $\Phi\xi \rightarrow 1/2$ for sufficiently small values of Y and Z which may occur for sufficiently high values of Ka^2. As a general tendency, with increasing Ka^2 the critical value $(\beta_c)/(p^{3/2}\xi^3)$ decreases and $\Phi_c\xi$ increases. For different values of Ka^2, results are shown

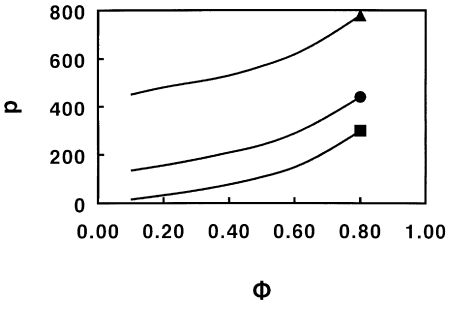

Fig. 4. Variation of number of aggregated cellulose molecules p with cellulose concentration Φ for different values of Ka^2. Others as in Fig. 2. Ka^2: 1 (■); 2 (●); and 4(▲).

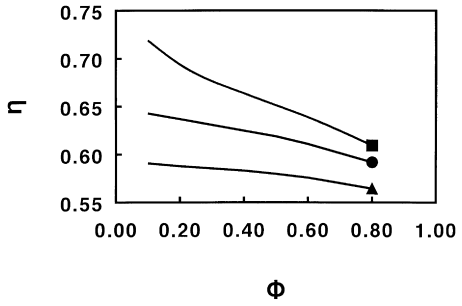

Fig. 5. Varation of reduced core length η with cellulose concentration Φ for different values of Ka^2. Markers as in Fig. 4.

in Fig. 6. With increasing Ka^2, the critical interaction parameter, $(\beta_c)/(\xi^3 p^{3/2})$, decreases. This implies that clustering becomes significant for high values of Ka^2 and attractions between the micelles may lead to phase instability of the particle phase. This clustering of the micelles generates a broad region in the phase diagram where a diluted solution coexists with a more concentrated solution. Strictly speaking, the two particle phases are not only different in overall cellulose concentrations but consist also of particles of different size. However, the differences in average numbers of molecules, aggregated in a micelle, are not significant. Therefore, the particle concentrations in the coexisting phases can be seen as $[\Phi/(pN_C)]\sim\Phi$ to a very good approximation. Fig. 6 also shows that with descending Ka^2, the critical interaction parameter more and more approaches Ka^2 which means that Eq. (13) becomes invalid.

4. Conclusions

Aggregates of the fringed micelle type can be stable in solutions. They are characterized by a highly ordered cylindrical core of aligned chains, which is insoluble in the solvent, and two spherical coronas surrounding the core ends. With respect to their solubility behaviour, the cellulose molecules, forming the aggregates, are seen as two different substances. As long as they are organized in ordered (crystalline) domains, they are completely insoluble in the solvent. In disordered regions on the other hand, they

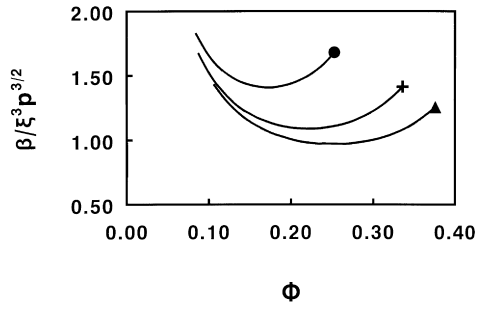

Fig. 6. Stability limits for cellulose solutions calculated after Eq. (15) with the parameters $N_C = 100$, $\nu = 1/2$, $a/d = 1$ and $\bar{\eta} = 0.6$. Ka^2: 2 (●); 3(+); and 4(▲).

are soluble. The aggregation of the chains, in a core, is driven by hydrogen-bond formation among the ordered cellulose molecules. In that way, the system can reduce the less favourable contacts with the solvent. However, as a result of the activation process, the ordered domains are surrounded by disordered regions which are soluble in the solvent and form the coronas. The number of chain molecules, forming the aggregate, and the thickness of the coronas increase with both interfacial tension between core and solvent and cellulose concentration in the system. Many-body attractions between the aggregates may lead to phase instability of the particle phase.

Finally, we have to mention that the suggested approach comprises crucial simplifications: (1) we assume a highly perfect fringed micelle, i.e. all the cellulose molecules, that form it, are perfectly aligned in a cylindrical core. This implies also that the coronas are perfectly spherical. These assumptions certainly simplify the reality. The molecules will be more or less dislocated in the core which results also in nonspherical coronas. (2) We assume that all particles are of the same size comprising p cellulose molecules. This means, we neglect the polydispersity of the particle phase that is likely to occur.

Appendix A

In a shell at distance r, from the end of the core, and thickness $\delta(r)$, there are p blobs of size δ:

$$r^2\delta \cong p\delta^3 \text{ or } \delta \cong \frac{r}{p^{1/2}} \tag{A1}$$

In general terms, the blob size is given by

$$\delta(r) = m(r)^{\nu} a \tag{A2}$$

where $m(r)$ is the number of monomers inside the blob at distance r and ν is the single chain exponent. With Eqs. (A1) and (A2), we get for the volume fraction of monomers inside the corona, $\Phi_{\text{corona}}(r)$, at distance r

$$\Phi_{\text{corona}}(r) \cong \frac{pm(r)a^3}{r^2\delta(r)} \cong p^{(3-1/\nu)/2}\left(\frac{a}{r}\right)^{(3-1/\nu)} \tag{A3}$$

As can be seen from Eq. (A3), $m = c\delta^3$, where c is the number density of monomers in the corona, $\Phi = ca^3$. Hence, the corona is a densely packed system of blobs. The thickness of the corona, H, follows from

$$a^3 p(1-\eta)\frac{N_C}{2} \cong \int_{R_c}^{R_c+H} r^2\Phi(r)\mathrm{d}r \cong \frac{\nu}{2^{1/\nu}} p^{3/2} a^3 \left(\frac{d}{a}\right)^{1/\nu} \times \left[\left(\frac{R_c+H}{R_c}\right)^{1/\nu} - 1\right] \tag{A4}$$

where Eq. (2) has been used. Then, we find

$$\left(\frac{R_c+H}{R_c}\right)^{1/\nu} \cong 1 + q\frac{(1-\eta)N_C}{p^{1/2}} \tag{A5}$$

where q is defined as in the context of Eq. (7). Since the blobs behave essentially as hard spheres, we may say that their energy equals k_BT. Then, one gets for the free energy of the spherical coronas (the surface energy of the coronas can be neglected)

$$\frac{\Delta F_{\text{corona}}}{k_BT} = 2\int_{R_c}^{R_c+H} dm_{\text{blob}} \cong 2\int_{R_c}^{R_c+H} \frac{r^2}{\delta^3}\mathrm{d}r \cong 2\nu p^{3/2} \times \ln\left[1+q\frac{(1-\eta)N_C}{p^{1/2}}\right] \quad \text{(A6)}$$

Appendix B

Minimization of Eq. (9) results in the following two equations (where one term, $1/pN_C\xi$, has been neglected)

$$1-\eta = \frac{1}{q}\frac{p^{1/2}}{N_C}\left[\frac{2^{1/\nu}}{\pi}\cdot\left(\frac{a}{d}\right)^{1/\nu+1}\frac{p^{1/2}}{\mathcal{K}}-1\right] \quad \text{(B1)}$$

and

$$\mathcal{K} = \frac{2\nu}{\pi}\left(\frac{a}{d}\right)\frac{p}{N_C}\ln\left[\frac{2^{1/\nu}}{\pi}\left(\frac{a}{d}\right)^{1/\nu+1}\cdot\frac{p^{1/2}}{\mathcal{K}}\right] - \frac{2}{\pi p^{1/2}N_C}\left(\frac{a}{d}\right)\ln(\Phi\xi) \quad \text{(B2)}$$

where q is defined as in the context of Eq. (7). Eq. (B2) is equivalent to

$$\frac{p^{1/2}}{N_C}\ln\left[1+q\frac{(1-\eta)N_C}{p^{1/2}}\right] = \frac{1}{\nu pN_C}\ln(\Phi\xi) + \frac{q}{1+q\dfrac{(1-\eta)N_C}{p^{1/2}}} \quad \text{(B3)}$$

Eqs. (B1) and (B2) allow us to compute $p(\Phi, Ka^2)$ and η if reasonable values of Ka^2, ν, (a/d) and N_C are known.

Appendix C

Explicit form of Y

$$Y = -\frac{2n}{n-1}\left(\frac{\Phi}{2p}\frac{\mathrm{d}p}{\mathrm{d}\Phi}\right) + \frac{2(n/2+1}{n-1}\left(\frac{\Phi}{2p}\frac{\mathrm{d}p}{\mathrm{d}\Phi}\right)^2 - \frac{1}{n-1}\left(\frac{\Phi^2}{2p}\frac{\mathrm{d}^2p}{\mathrm{d}\Phi^2}\right) \quad \text{(C1)}$$

Derivatives of p with respect to Φ

From Eq. (B1), we have

$$S[Ka^2 - 1 - \ln(1-\Phi\xi)] = \frac{2^{1/\nu}}{\pi}\left(\frac{a}{d}\right)^{1/\nu+1}p^{1/2} \quad \text{(C2)}$$

with

$$S \equiv 1 + q\frac{(1-\eta)N_C}{p^{1/2}} \quad \text{(C3)}$$

Eq. (C2) leads to

$$\left(\frac{\Phi}{2p}\frac{\mathrm{d}p}{\mathrm{d}\Phi}\right) = \frac{S}{S-1}\frac{\Phi\xi}{1-\Phi\xi}\frac{1}{\left[\mathcal{K}+\dfrac{2\nu}{\pi}\left(\dfrac{a}{d}\right)\dfrac{p}{(1-\eta)N_C}\right]} \quad \text{(C4)}$$

We now assume that $N_C/p^{1/2} \gg 1$ then it follows $S/(S-1) \approx 1$ and in the same approximation (from Eq. (B1))

$$\mathcal{K} \approx \frac{2\nu}{\pi}\left(\frac{a}{d}\right)\frac{p}{(1-\eta)N_C}$$

Using these approximations, Eq. (C4) becomes Eq. (18). Starting from Eq. (C4), one can calculate the second derivative of p with respect to Φ and eventually, one gets in the same approximation the second derivative given in Eq. (18).

References

[1] Turbak AF. Tappi J 1984;67:94.
[2] Vollbracht L. Chemiefasern/Textilind 1989;39/91:935.
[3] Philipp B. J Macromol Sci, Pure Appl Chem 1993;A30:703.
[4] Morgenstern B, Kammer HW. Trends Polym Sci (TRIP) 1996;4:87.
[5] Turbak AF, El-Kafrawy A, Snyder FW. Auerbach AB. (ITT Corp.), US Patent No. 4,302,252. 1981.
[6] Schleicher H, Loth F, Lukanoff B. Acta Polymerica 1989;40:170.
[7] Burchard W. Trends Polym Sci (TRIP) 1993;1:192.
[8] Schulz L, Burchard W. Das Papier 1993;47:1.
[9] Asahara T, Ikeda K, Yoda N. J Polym Sci, Polym Chem 1968;6:2489.
[10] Balasubramanian D, Shaikh R. Biopolymers 1973;12:1639.
[11] El-Kafrawy A. J Appl Polym Sci 1982;27:2435.
[12] Saint-Germain J, Vincendon M. Organ Magn Res 1983;21:371.
[13] McCormick CL, Callais PA, Hutchinson BH Jr. Macromolecules 1985;18:2394.
[14] Morgenstern B, Kammer HW, Berger W, Skrabal P. Acta Polymerica 1992;43:356.
[15] Halperin A. Macromolecules 1990;23:2724.